Published online 23 October 2008 *Nucleic Acids Research, 2008, Vol. 36, No. 21* ***6739–6751***
doi:10.1093/nar/gkn775

Aptamers that recognize drug-resistant HIV-1 reverse transcriptase

Na Li, Yuxuan Wang, Arti Pothukuchy, Angel Syrett, Naeem Husain, Siddharth Gopalakrisha, Pradeepa Kosaraju and Andrew D. Ellington*

Department of Chemistry and Biochemistry, Institute for Cell and Molecular Biology, University of Texas at Austin, Austin, TX 78712, USA

Received July 18, 2008; Revised October 7, 2008; Accepted October 8, 2008

ABSTRACT

Drug-resistant variants of HIV-1 reverse transcriptase (RT) are also known to be resistant to anti-RT RNA aptamers. In order to be able to develop diagnostics and therapies that can focus on otherwise drug-resistant viruses, we have isolated two aptamers against a well-known, drug-resistant HIV-1 RT, Mutant 3 (M3) from the multidrug-resistant HIV-1 RT panel. One aptamer, M302, bound M3 but showed no significant affinity for wild-type (WT) HIV-1 RT, while another aptamer, 12.01, bound to both M3 and WT HIV-1 RTs. In contrast to all previously selected anti-RT aptamers, neither of these aptamers showed observable inhibition of either polymerase or RNase H activities. Aptamers M302 and 12.01 competed with one another for binding to M3, but they did not compete with a pseudoknot aptamer for binding to the template/primer cleft of WT HIV-1 RT. These results represent the surprising identification of an additional RNA-binding epitope on the surface of HIV-1 RT. M3 and WT HIV-1 RTs could be distinguished using an aptamer-based microarray. By probing protein conformation as a correlate to drug resistance we introduce an additional and useful measure for determining HIV-1 drug resistance.

INTRODUCTION

HIV-1 RT is a primary target in the generally accepted highly active antiretroviral therapies (HAARTs) used in the treatment of AIDS (1). Twelve of 25 anti-HIV drugs approved by the FDA inhibit the DNA polymerase activity of HIV-1 reverse transcriptase (RT). These drugs can be further classified as nucleoside analog RT inhibitors (NRTI) and non-nucleoside RT inhibitors (NNRTI). The NRTI drugs lack 3′-hydroxyl moieties and function as DNA chain terminators, while the NNRTI drugs allosterically inhibit RT polymerase activity. In HAART, multiple anti-HIV drugs including both NRTI and NNRTI drugs are used in order to reduce the probability of the evolution of viral resistance.

However, drug resistance mutations that can inactivate many of the anti-RT compounds are still found to arise regularly (2), primarily because the process of reverse transcription involves no proofreading mechanism. The mutation rate of HIV-1 RT has been determined to be 3.4×10^{-5} per nucleotide per replication cycle (3). Considering that ~10 billion (10^{10}) HIV-1 virions are produced daily in an infected individual (4), viruses with almost every possible single mutation as well as most of the double mutations are expected to be readily generated. The development of drug-resistant viruses in patients quickly leads to the failure of HAART (5). Indeed, the proportion of drug-resistant strains in new HIV-1 infections detected by sequence analysis rose from 8.0% in 1995–98 to 22.7% in 1999–2000 in North America (6). It was similarly reported that the prevalence of the transmission of drug-resistant HIV-1 rose from 13.2% in 1995–98 to 24.1% in 2003–04 in New York City (7). With the increasing prevalence of drug resistance, it is of great necessity to develop both new antiretroviral drugs that can target mutant HIV-1 RTs and also low-cost diagnostic assays capable of identifying drug-resistant forms of HIV-1 RT and thereby guiding therapies.

Aptamers are nucleic acid-binding species selected *in vitro*, and have proven to be as good as monoclonal antibodies for distinguishing between protein targets. In particular, numerous RNA and DNA aptamers have been isolated that target wild-type (WT) HIV-1 RT (8). The first HIV-1 RT aptamer was isolated in the Gold lab from an RNA pool that spanned a 32-nt random region (9). The selected aptamers folded into a pseudoknot structure and bound RT with dissociation constants in the low nanomolar range. Additional RNA aptamers against WT HIV-1 RT have since been selected from N70 and N80 pools (10). These aptamers formed either pseudoknot or stem–loop structures, and again bound WT HIV-1 RT in the low nanomolar range. DNA aptamers against HIV-1

*To whom correspondence should be addressed. Tel: +1 512 471 6445; Fax: +1 512 471 7014; Email: andy.ellington@mail.utexas.edu

RT have also been selected, and appear to form hairpins, pseudoknots (11) and G-quartets (12).

While WT HIV-1 RT is bound by these aptamers, little was known about how anti-RT aptamers interacted with drug-resistant RT variants. Pseudoknot-like anti-RT RNA aptamers expressed *in vivo* have been shown to be effective against HIV-1 subtypes A, B, D, E and F, but more poorly inhibited subtypes C and O and the chimera A/D (13). The RNA aptamers shown to inhibit HIV strains were known to be resistant to AZT, 3TC, ddI, ddC and nevirapine. However, the binding properties of the aptamers *in vitro* were unknown, as was the correlation between binding *in vitro* and activity *in vivo*. More recent studies have shown that DNA anti-RT aptamers can inhibit an even broader range of RT variants *in vitro* (including HIV-1, HIV-2 and simian immunodeficiency virus SIV_{cpz}), which are again known to have varying drug sensitivities (14,15). The DNA anti-RT aptamer RT1t49 folds into a stem–loop structure and binds to the template-primer cleft of RT (16). This aptamer has proven to be synergistic with NRTIs (AZTTP or ddCTP) but additive with NNRTIs (Nevirapine or Efavirenz), at least *in vitro* (15).

Just as drug-resistant mutations can arise, aptamer-resistant variants of HIV-1 RT have been shown to occur. Two mutants (N255D and N265D) of HIV-1 RT were found that were resistant to the DNA anti-RT aptamer RT1t49 (15). These two mutations did not promote resistance to either NRTIs or NNRTIs, but did affect the majority of anti- RT aptamers being tested (17). Natural variants of HIV-1 RT also show resistance to some aptamers; the substitution R277K that occurs in some RT variants yields resistance against some RNA pseudoknot aptamers (14).

Because sequence variants of RT evade some anti-RT aptamers and additional sequence variants that would defeat aptamers may arise, it would be useful to have aptamers against specific RT variants. For example, we find that the canonical pseudoknot RNA anti-RT aptamers do not bind *in vitro* to HIV-1 RT variants resistant to NRTIs, but that we can isolate novel aptamers that bind to these drug-resistant variants. Moreover, our aptamers can bind to novel epitopes on both the WT and mutant proteins, ultimately allowing both broad and specific detection of HIV-1 RT variants. Traditional antiretroviral resistance assays detect either the phenotype (viral replication) or the genotype (sequence) of HIV-1 RT (5). Phenotyping assays directly and quantitatively measure the drug resistance of HIV-1 RT and can be used with plasma samples that have viral loads of about 500 HIV RNA copies/ml. However, phenotyping assays are relatively involved and hence expensive and slow, with a turnaround time of about 2–4 weeks. Genotyping assays have similar sensitivities and detection ranges, are less expensive, and have turnaround times of <1 week (18). However, genotyping requires a foreknowledge of drug-resistant alleles, and the interpretation of how sets of alleles map to resistance profiles may be nonobvious. Even though these assays have been widely adopted in standard HIV care, they are both laborious and expensive. We believe that since our aptamers can specifically detect purified HIV-1 RT in complex biological fluids at concentrations as low as 1 nM, they may prove useful in diagnostic methods such as aptamer-based microarrays (19,20) both for directly typing HIV-1 RT drug-resistant variants and for augmenting genotyping assays.

MATERIALS AND METHODS

HIV-1 RT preparation

Wild-type HIV-1 RT was purchased from Ambion (Austin, TX) and Mutant 3 (M3) HIV-1 RT was prepared as previously described with some minor modifications (21). In short, the p51 subunit was cloned into the vector pET30a (+) and the p66 subunit was cloned into pET21a (+). The two subunits were expressed separately in a BL21 (DE3) codon plus RIL *Escherichia coli* strain (obtained from Novagen, Gibbstown, NJ). The heterodimeric M3 HIV-1 RT was purified on a DEAE-Sepharose (Promega, Madison, WI) column followed by a Ni-affinity column (Qiagen, Valencia, CA). Pellets of p66 and p51 were resuspended in Buffer A [50 mM Tris–HCl, pH 7.9, 60 mM NaCl, 8% glycerol (v/v), and 1 mM dithiothreitol (DTT)] at a 4:1 molar ratio (four parts p66 to one part p51) and pooled. Cells were disrupted using a flow-through, high-pressure homogenizer and then centrifuged at 28 000×*g* for 45 min at 4°C. Supernatants were loaded onto DEAE-Sepharose columns equilibrated with Buffer A. The gravity flow-through was collected, pooled, supplemented with NaCl to 500 mM and imidazole to 10 mM, and then loaded onto Ni–NTA columns pre-equilibrated with Buffer B [50 mM Tris–HCl, pH 7.9, 500 mM NaCl, 8% glycerol (v/v) and 1 mM DTT] supplemented with imidazole to 10 mM. The columns were washed with 12 column volumes (CV) of Buffer B with additional NaCl to 1M, 12 CV of Buffer B with 5 mM imidazole and 12 CV of Buffer B with 10 mM imidazole. RT was sequentially eluted with single CV of Buffer B supplemented with 40 mM, 60 mM, 100 mM and 200 mM imidazole. Eluted fractions were assayed for purity by SDS–PAGE. Fractions were pooled according to purity (>97%) and then dialyzed overnight into 2 × Storage Buffer (50 mM Tris pH 7.5, 150 mM NaCl, 20% glycerol and 1 mM DTT) using 3-ml Slide-a-lyzer dialysis cassettes (Pierce, Rockford, IL) with a 3500 MWCO. RT samples were frozen at –20°C and used within 4–6 weeks, or frozen at –80°C for longer-term storage. Protein concentrations were determined using a Bradford Assay (Bio-rad, Hercules, CA).

In vitro selection

The DNA library for selection consisted of a 50-nt random region flanked by two primer sequences: 5′-gata atacgactcactatagggttacctaggtgtagatgct-N_{50}-aagtgacgtctga actgcttcgaa-3′ (T7 RNA polymerase promoter is underlined). Some 10^{13} DNA templates were transcribed *in vitro* by T7 RNA polymerase to generate the initial pool RNA (*ca.* 100 copies of each member of the pool). After transcription, DNA templates were digested with DNase and the transcripts were gel-purified and ethanol-precipitated. A negative selection against the filter alone

was carried out by incubating the RNA in Selection Buffer (200 mM NaCl, 50 mM Tris–HCl, pH 7.4, 10 mM DTT and 6 mM $MgCl_2$) and then passing it through 0.45 μm modified cellulose disks (Millipore, Bedford, MA). M3 HIV-1 RT was added to the negatively selected RNA pool at a final concentration of 500 nM in the first three rounds, 200 nM for the next three rounds and 50 nM for the remaining rounds of selection. The binding reaction was incubated at 25°C for 10 min and then filtered through 0.45 μm modified cellulose disks. After washing with 1 ml Selection Buffer, bound species were eluted from the modified cellulose membranes by incubating in Elution Buffer (200 mM NaCl, 25 mM EDTA and 8 M urea) at 95°C for 5 min. Recovered RNA was reverse-transcribed and PCR-amplified to generate DNA templates for the next round of selection. The selected pool from round 12 was cloned and sequenced according to standard procedures.

Doped selections were carried out under similar conditions, except that the negative selection was against WT HIV-1 RT. The concentrations of M3 and WT HIV-1 RTs were 260 nM for the first round, 40 nM for the second round and 10 nM for the last six rounds.

Aptamer secondary structures and boundaries

The modification of RNA with NMIA (*N*-methyl-isatoic anhydride) and primer extension of modified RNA were done as previously described for SHAPE (Selective 2′-Hydroxyl Acylation and Primer Extension) (22). To determine the 3′-boundary of active M302, (5′-^{32}P)-labeled RNA was digested with 0.05 U/μl of RNase T1 (Ambion, Austin, TX) to generate a size marker [6 min at 50°C in 20 mM NaAc (pH 5.2), 10 mM EDTA and 1 μg tRNA]. End-labeled RNA was also partially hydrolyzed (5 min at 90°C in 50 mM $NaHCO_3$ and 1 μg tRNA) to generate RNA fragments, which were EtOH-precipitated. A small portion of the recovered RNA fragments was saved to serve as an RNA fragment ladder. The rest was incubated with 500 nM of M3 HIV-1 RT for 10 min at 25°C. Active RNA fragments were caught on modified cellulose and separated from inactive ones. Recovered RNA fragments from modified cellulose filtration were fractionated on an 8% denaturing polyacrylamide gel along with the RNA fragment ladder and RNase T1 marker. For 5′-boundary determination, (3′-^{32}P)-labeled RNA was prepared by the addition of an α-^{32}P ddATP to its 3′-end by poly(A) polymerase. The 3′-end-labeled RNA was then treated similarly to the 5′-end-labeled RNA described above. Based on the boundary experiments and predicted RNA secondary structure, three shorter versions of M302 and 12.01 were designed and prepared by transcription from the T7 RNA polymerase phi 2.5 promoter on foreshortened DNA templates. Since the phi 2.5 promoter was used, all six transcripts began with AG and ended with CU.

Binding constants and specificities

The dissociation constants of isolated aptamers were determined by plotting the fraction of RNA bound to the nitrocellulose filter as a function of protein concentration, using the following equation:

$$\text{RNA Bound} = \frac{B_{max}\,[\text{Protein}]}{K_d + [\text{Protein}]},$$

where B_{max} is the extrapolated maximal amount of RNA:protein complex that will be bound. The binding reaction was carried out by incubating 0.1 nM (5′-^{32}P)-labeled RNA with 1, 3.2, 10, 32, 100, 320 and 1000 nM of protein in Selection Buffer for 10 min at 25°C. To separate the RNA bound to protein from free RNA, the binding reaction was sieved through filters (Schleicher & Schuell, Keene, NH) on a vacuum manifold. The first filter layer was nitrocellulose (top) and captured only the RNA:protein complexes, while the second filter layer was nylon (bottom) and captured all remaining RNA. After washing with 1 ml of Selection Buffer, nitrocellulose and nylon filters were dried and visualized via a Phosphorimager (GE Healthcare, Piscataway, NJ).

The dissociation constant of TPK1.1 was measured under the same conditions that it was selected under (RNA and protein were mixed and stored on ice for 30 min and then transferred to 37°C for 5 min in 200 mM KOAc, 50 mM Tris–HCl, pH 7.7 and 10 mM DTT). Aptamers M302 and M302-S were labeled during transcription with [α-^{32}P]-ATP (3000 Ci/mmol, 10 mCi/ml, Perkin Elmer, Waltham, MA) and incubated separately with 0.5 μM of M3 HIV-1 RT, WT HIV-1 RT (Ambion), AMV RT (Promega) or M-MLV RT (Invitrogen, Carlsbad, CA) in Selection Buffer for 10 min at 25°C.

Inhibition assays

RNA templates for reverse transcription = 5′ GGGGAA UUGUGAGCGGAUAACAAUUCCCCUCUAGAAA UAAUUUUGUUUAACUUUAAGAAGGAGAUAUA CCAUGGGCAGCAGCCAUCAUCAUCAUCAUCAC 3′ were transcribed from dsDNA which was amplified from a PET28 vector (Invitrogen) with the following primers: forward primer = 5′ CGCGAAATTAATACGA CTCACTATAGGGGAATTGTGAGCGG 3′, and reverse primer = 5′ GTGATGATGATGATGATGGC TGCTGC 3′. A stock template:primer mix (5X) was prepared by denaturing 25 nM 5′-end-labeled reverse primer and 125 nM RNA template in Selection Buffer (minus DTT) at 70°C for 3 min and slowly cooling (at 1°C/s to room temperature. The polymerase activity of WT and M3 HIV-1 RTs was assayed by incubating a 5 nM template:primer mix with 50 μM of dNTPs and RT (15, 50 and 500 nM) in Selection Buffer at 37°C for 10 min. As a positive control for inhibitory activity, extension reactions were performed in the presence of different concentrations of the TPK1.1 aptamer. Different concentrations of aptamers (50 nM, 200 nM and 1000 nM) were added to the reactions containing 50 nM of either WT or M3 HIV-1 RT. Reactions were quenched by adding 20 mM EDTA. cDNAs were separated from unextended reverse primers by 8% PAGE and quantitated using a Phosphorimager.

RNase H activity was assayed by incubating 5 nM template:primer mix with RTs (15, 50 and 500 nM) in Selection Buffer at 37°C for 10 min. The template:primer mix for the RNase H assay was prepared similarly to that described above except that 125 nM unlabeled reverse primer and 25 nM 5′-end-labeled RNA template were used. Reactions were analyzed by gel electrophoresis and quantitation, as with the polymerase assay.

Competitive binding assay

Competitions between unselected pool RNA, M302, 12.01 and TPK1.1 for HIV-1 RTs were carried out by mixing 100 nM of M3 HIV-1 RT with 1 μM of each unlabeled RNA (pool RNA, M302, 12.01 and TPK1.1, respectively) in Selection Buffer followed by the addition of ~0.1 nM of (5′-^{32}P)-labeled M302. The reaction was incubated for 10 min at 25°C. Binding assays of (5′-^{32}P)-labeled 12.01 with M3 HIV-1 RT, (5′-^{32}P)-labeled 12.01 with WT HIV-1 RT and (5′-^{32}P)-labeled TPK1.1 with WT HIV-1 RT were all carried out under the same conditions. Protein-bound RNA and free RNA were separated on a vacuum manifold, and visualized via a Phosphorimager as described for the measurement of aptamer dissociation constants.

Microarray analysis

Biotinlyated RNA was transcribed from templates containing the T7 RNA polymerase phi 2.5 promoter and biotin-AMP (Biotin-8; Adegenix, Monrovia, CA). After purification, biotinlyated RNA was resuspended in Selection Buffer, heated to 70°C for 3 min and slowly cooled to 25°C. Glycerol was added to the samples to a final concentration of 5%. Biotinlyated RNA was printed onto neutravidin-coated slides (Pierce) using a Manual Glass Slide Microarrayer (V&P Scientific, San Diego, CA) at 65–75% humidity, and the slides were incubated for an additional 30 min. The slides were then covered with a 16-well Flexwell partitioning pad (Grace BioLabs, Bend, OR) for the addition of solutions. The surface of the neutravidin-coated slide was blocked with Blocking Buffer [1× Selection Buffer with 1× Roche blocking buffer and 0.1% Tween-20 (Sigma Aldrich, St Louis, MO)] for 45 min at room temperature. After rinsing three times with 100 μl Blocking Buffer, the samples were incubated with 75 μl of 1 nM target protein suspended in Blocking Buffer for 45 min at room temperature. The wells were rinsed six times with 100 μl Blocking Buffer before application of the primary antibody (100 μl, 1:6000 dilution in Blocking Buffer). After 2 h incubation, the wells were rinsed six times with 100 μl Blocking Buffer. The secondary antibody (100 μl, 2 μg/μl in Blocking Buffer) was applied to each well and incubated for 1 h, followed by six rinses with 100 μl Blocking Buffer. The primary antibody was an anti-HIV-1 RT polyclonal from rabbit, obtained from Dr. Stuart Le Grice through the NIH AIDS Research and Reference Reagent Program, Division of AIDS, NIAID, NIH. The secondary antibody was a polyclonal Cy3-labled goat anti-rabbit IgG and was purchased from Amersham Biosciences (Piscataway, NJ). The slide was further rinsed sequentially with 40 ml of Blocking Buffer, Selection Buffer with 0.1% Tween-20, and Selection Buffer in a 50 ml conical tube for 5 min each with shaking. The Flexwell was peeled off and the slide was spin-dried and gently dried with hot air. The processed slide was then immediately scanned on a microarray scanner—GenePix 4000 B (Molecular Devices, Sunnyvale, CA).

RESULTS AND DISCUSSION

In vitro selection of aptamers that bind to drug-resistant HIV-1 RT

An RNA library with a N50 random region was used as a starting point for the isolation of aptamers that specifically bind to a mutant HIV-1 RT, M3 from the panel of 12 prototypical multidrug-resistant HIV-1 RT clones (23; mapped to the RT structure in Figure 1). This mutant RT was found to be highly resistant to the nucleoside RT inhibitor 3TC (Lamivudine) and moderately resistant to AZT (Zidovudine), ABC (Abacavir), ddI (Didanosine), d4T (Stavudine) and TDF (Tenofovir) (24). It contains 8-amino-acid substitutions relative to the WT. Among them, M41L, D67N, L210W and T215Y belong to the set of thymidine analog mutations (TAMs) and account for the resistance to AZT (25,26). The E44D and the V118I mutations are strongly associated with TAMs and in combination with the mutations cited above confer dual resistance to AZT and 3TC (27,28). The substitution M184V evokes not only strong resistance to 3TC, but also some loss of resistance to AZT (29–31).

Aptamer selection was carried out for 12 rounds via filtration of the protein-bound population on a modified cellulose filter (32). The progress of the selection was monitored every other round by assaying the amount of RNA retained on the modified cellulose filter relative to the total filtered population. Binding species increased from 2% in Round 0 to 17% in Round 10 and 19% in Round 12. During the course of the selection, a negative selection against the filter alone was included to insure that filter-binding species were not enriched. Further selection resulted in decreased pool binding affinity to M3 HIV-1 RT. Thus the Round 12 population was used in further analysis and diagnostic testing.

Some 29 clones from Round 12 were sequenced (Figure 2a). Most of the sequences in the population appeared to differ substantively from one another except for Aptamer 12.01, which was repeated five times. In order to better identify common sequence motifs, we chose to use the MEME server (http://meme.sdsc.edu), which discovers motifs in groups of related DNA sequences using statistical modeling techniques (33). No common sequence motifs were found that could be used to subdivide the population into sequence families.

An initial binding analysis showed that Apatmer 12.01 bound to both M3 and WT HIV-1 RTs with similar binding affinities. In a further attempt to isolate aptamers that would more specifically bind to M3 HIV-1 RT, a partially randomized population centered on Aptamer 12.01 was generated. This 'doped'sequence pool contained 70% WT residues and 30% non-WT residues (i.e. 70% G,

	WT	M3
41	M	L
44	E	D
67	D	N
69	T	D
118	V	I
184	M	V
210	L	W
215	T	Y

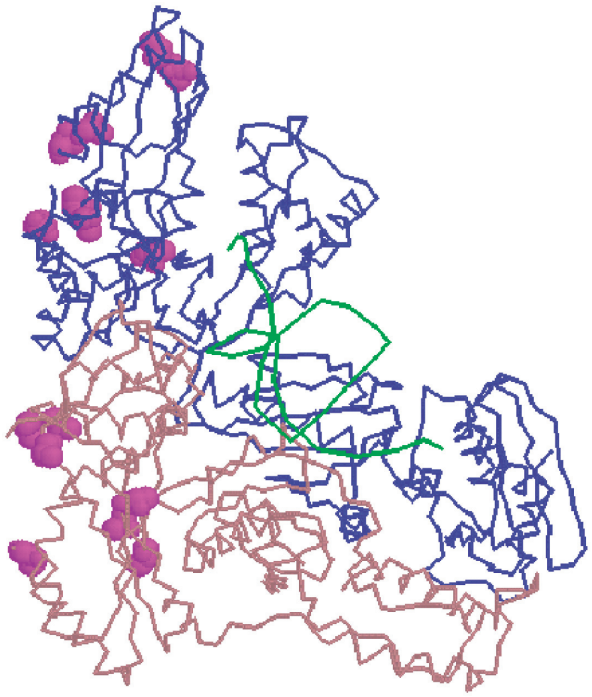

Figure 1. Drug resistance mutations in M3 HIV-1 RT. (**a**) Sequence substitutions of M3 (right) relative to WT (left). Numbers indicate position in the amino acid sequence. (**b**) Sequence substitutions in M3 HIV-1 RT (pink) mapped onto the known 3D structure. The chain in blue is the WT HIV-1 RT p66 subunit and the chain in magenta is the p51 subunit. A 33 residue, pseudoknot RNA aptamer that interacts with the RT template/primer-binding site is shown in green. This image was generated through Protein Explorer using the 1hvu PDB file as a template.

(**a**)

Clone	Sequence	Repeats
12.01	CUUCAGAUUCAUUUAUAAGAUCCGACAACCUGUCUAUUAGUUGCGCCGAUU	5
12.02	AACUCAUUGGGAGUCGUGUAAAGCAUCCGCCCUUCCUUUCCUCACCGGCU	1
12.03	AGUCCGCUGCUUAGCUCAUAAGUGUUUGCCCCUCCACAAUUCGCCAAAA	1
12.04	AGCCUGCAAAACUCUCAAUGUAGGUAUAGGCUAACAUUCCCGGGCGCUGC	1
12.05	CGCAUACCUUCGCAUUCGCUGGCCCCUAUUUUUUAGCCUCGUACCUCAGU	1
12.06	UAAGCUAAAAAUAACAAUAAAAUUAACAACUGACACCCGGUUCGAUCGUA	1
12.07	AUAUUCUUACUCCUCUUUACGAAAGAUCUAUCUAAUAUCACUACGCGGC	1
12.08	AUUCUUGUCUAUCUUUCAAAAUACCAAUUCUUGACGCCCAAUUACUCGCC	1
12.09	CACUUACACAAACCUGUAGUUUUAUGCUUCACAUAUCGCACAGGACGCUU	1
12.10	UACUCAAUUUCUCGAAGUUCUAAUUAAUUACAGACUCUCGCCGCAGCUUC	1
12.11	GAUAUUCGCAUUGGCUUCGUCUCAUUUUUAAAUUUUCUGCGGAUCGCAAGC	1
12.12	CAUGUGAGGCACUGAAGCUUAGAUUGUCGUUCCCCUUGGCCCAUCCAUAU	1
12.13	CAUAUCGGCGUGCAAUGACGCUCCUUAAACACCUCCGUUGACAUGGCCG	1
12.14	CACAAAUCUUACGCUGCGCCACUCCCCCCUGCCAAGCUUCAAAGUGGUG	1
12.15	UUUUGCCCGGCUUGGCACAUUCAGAAGGGAACGGACUACCCGCGGUUCUGU	1
12.16	UCCACGAGCCAACAUGUUCUUUGCACAAUUAGUUCCACGCAUUCCUCUGU	1
12.17	UUUUUCACUCGCUCGUUUUUUAGCGCAACAUCAAAAUUGGUUGUCUCGGC	1
12.18	CGAUGCGCUUUGUACUACACAUAUGGACAGCUCACACCCCUUCGCCUU	1
12.19	CGCAGCUCCUUCCUCAUUCCAGAUUGUCGUAAUUCAUCCCAUUGCUCCCC	1
12.20	ACGGCUGUUAGAAUGUGCCGUCACAAAGUAUAGGUUAGCGCGCCUGCAA	1
12.21	AGCUCUGCUAUCUGGCGUACAAAUUUGCCCAUCGCCUCGUAGUUUCGUGC	1
12.22	UAACAUAGUUGUCGAAGUCCUUUGUAAGUGGGCUUCCAUAGCUACCAUUU	1
12.23	UAAACAAUUCUAAUAAAAUCGCACUACUUCGGCAUCAAACCCAUCGAUGC	1
12.24	GCAAAGUGAUACGUUAAGUCUUUUUAAUCACAUGUAUAGCUCACCCGCAU	1
12.25	CUUCCCUCCUCCACAAAUUAUUUUCUUUGACCACCCGCCCAUCGAACGCC	1

(**b**)

Clone	Sequence	Repeats
12.01	CUUCAGAUUCAUUUAUAAGAUCCGACAACCUGUCUAUUAGUUGCGCCGAUU	4
M302	CACUUACACAAACCUGUAGUUUUAUGCUUCACAUAUCGCACAGGACGCUU	4
M303	GAUAUUCGCAUUGGCUUCGUCUCAUUUUUAAAUUUUCUGCGGAUCGCAAGC	2
M304	UAACAUAGUUCUCGAAGUCCUUUGUAAGUGGGCUUCCAGAGCUACCAUUU	1
M305	AUAGCAUUAAGCAUCGUCCUUUUACACACGCUUACAAGUUUGCGACCUCC	1
M306	UAACAUAGUUCUCGAAGCCCUUUGUAAGUGGGCUUCCAGAGCUACCAUUU	1
M307	CACAUCCCAUUCAACCGGCGCUGGCAAUUUCUUCCCUACAGAUAUCGUGC	1
M308	AUCUCCAAAUUCCCUUAAGUACUUGCCCGAUAAAUUUGUUCGCCAUGGGU	1
M309	UGGUAGGCACAUGUAUACCUCAGAUAGUUACAAGUCACACCCCGAGCGAC	1
M310	UGAGAUAUCGUAAACGCUAAAUCUUCCUCGUGAAAGUUUGCAUCUCCUUC	1
M311	AGACGUUUUGUGUUAGUCGCCGUCCAACGUCUUUCAGCUAAUUCAUCGAU	1
M312	UGUGCUUGCCGGAUAUGGUUCAGAUUUCUUGAUAUGAAACACCCUUUGCC	1
M313	AAUGAUAGUUAGUCAAGGUUCUGUCAGACAUCCUUGCAAGGGCCAGCUC	1
M314	UAUUGCGCACUCAAAGGACGAAACCCGUACCUAUGCGCUGUAAAUUGUUC	1
M315	CUGAUGGAAUGUUCAUUUUCUGUAAUUAGAUGUGCGAGUGGCUGGCCAAUC	1
M316	UAAGAUAACUACGGCGAGUAAAACUAUAAAAAGAGUCGUAAGUCCUGUCUC	1
M317	UUACAACCAUAAAUUUUACCGCAUACGCCGCAUUUCCAACUGCUCUCAUC	1
M318	UGAUAAUUUGGUAUGCGACCCUCAUCCCUUAGCGUCUCUCGACUGAAUCC	1
M319	UCAUGGGAUAAACUCGCCAUAAACAAUAAUUAUAAACAAAGACAUGGCAA	1
M320	UAUUGCGCACUCAAAGGACGAAACCCGUACCUGUGCGCUGUAAAUUGUUC	1
M321	ACUUUACAGCGUAGAGCGUUAUGUCCCGGUAAAUCAUCCAUAGCGACUCU	1
M322	AUUUAUAUUAUGCAUUGCUGGUUUAUUUAGCUAUUGCAUAACCAUUGACA	1
M323	GCAAAGCGAUUAACACGCAUGUAUAGCUCCCACCCCAAUAUGCAGCGUUC	1

Figure 2. Sequences of aptamers binding to M3 HIV-1 RT. (**a**) Sequences from 29 clones isolated from the selected Round 12 pool that bound to M3 HIV-1 RT. The constant regions are not shown. The number of repeats of each sequence is shown to the right. (**b**) Sequences from 30 clones isolated from the selected Round 8 doped Aptamer 12.01 pool that bound to M3 HIV-1 RT. Repeats are again indicated to the right. Sequence M302 from the previous selection was found again in this selection, likely indicating a small amount of cross-contamination.

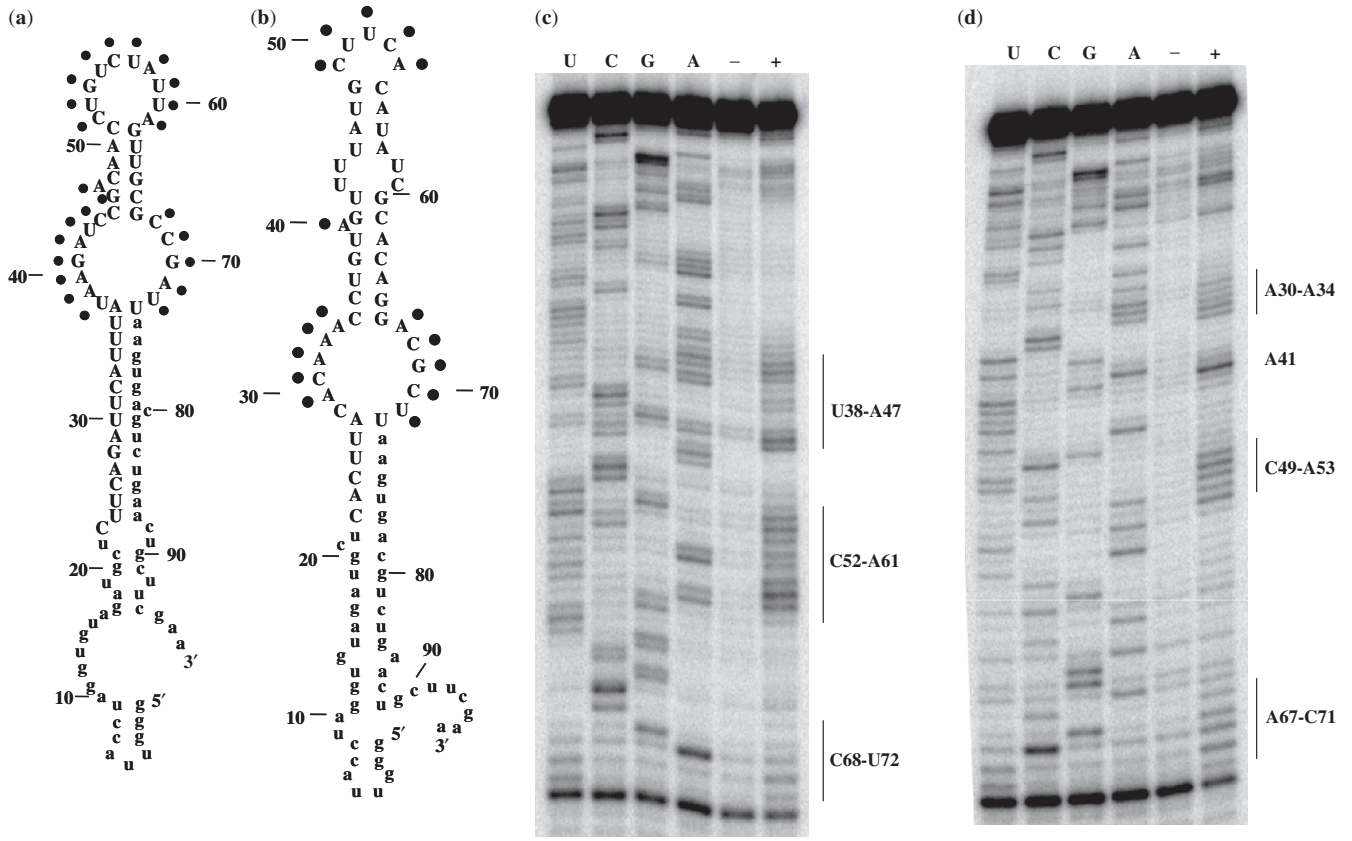

Figure 3. Secondary structural analysis of aptamers. (**a**) Predicted secondary structure of Aptamer 12.01. Numbers are nucleotide positions relative to the 5′-end of the RNA (+1). The dots are nucleotides whose 2′-hydroxyl groups are available for NMIA-modification as revealed by SHAPE. (**b**) Predicted secondary structure of Aptamer M302. Numbers and dots are the same as in (a). (**c**) Probing the secondary structure of Aptamer 12.01 using SHAPE. Lanes 'U', 'C', 'G' and 'A' are dideoxy-sequencing ladders. The lane marked as '+' is transcription-mediated primer extension of NIMA-modified Aptamer 12.01. Bands are offset by 1 nt compared to the sequencing ladder. Nucleotide positions corresponding 2′-O-adduct formation are numbered according to NMIA lanes and were marked in the predicted secondary structure for Aptamer 12.01, shown in (a). The lane marked as '–' is primer extension of unmodified Aptamer 12.01. (**d**) Probing the secondary structure of Aptamer M302 using SHAPE. Modified positions were marked in the predicted secondary structure for Aptamer M302, shown in (b). Conventions are as in (c).

10% A, 10% U and 10% C) at each originally random sequence position. Eight additional rounds of selection were carried out; in each round a negative selection against WT HIV-1 RT was included, effectively removing as many WT binding species from the population as possible. The selection yield increased from 2% (Doped 12.01, Round 0) to 25% (Round 8) for M3 HIV-1 RT and at the same time from 1% (Doped 12.01, Round 0) to 10% for WT HIV-1 RT (Round 8). It is interesting that despite the negative selection that there was some residual affinity for the WT HIV-1 RT, indicating that the identification of aptamers that can discriminate based on the few mutations that distinguish these proteins is a relatively difficult task. The binding affinities of the Round 7 pool and Round 8 pools were similar, and thus the selection was considered to be complete.

A total of 30 clones from the selected, doped pool were sequenced. The parental Aptamer 12.01 was found to occur multiple (four) times, as did the Aptamer M302 (four times) and M303 (two times) (Figure 2b). Sequence M302 was also present once in the previous selection, indicating that it may have entered the selection as a contaminant. Again, no common sequence motifs were found between any of the aptamers. Since no consensus families or motifs were apparent, we carried out further analyses with Aptamers 12.01 and M302, as these were the sequences that were most prevalent in both selections.

Structural analyses of selected aptamers

Many of the previously isolated RNA aptamers against HIV-1 RT fold into pseudoknot structures (9,10). Aptamers 12.01 and M302 are predicted to fold into stem–loop structures (34) (Figure 3a and b). However, since MFOLD cannot predict pseudoknot structures with accuracy, we attempted to confirm the predicted structures using the SHAPE method (Figure 3c and d) (22). In this method, the 2′-hydroxyl groups of flexible nucleotides (for example, those in loop regions) can react with NMIA to form a nucleotide 2′-ester, which is in turn revealed by primer extension. In contrast, nucleotides in base-paired regions are frequently unreactive to modification. Since RT stops at the nucleotides just prior to the 2′-O-adduct (35), the bands from NMIA are 1 nt off from the dideoxy sequencing ladder. In Figure 3, the nucleotide positions are numbered according to the NMIA lanes.

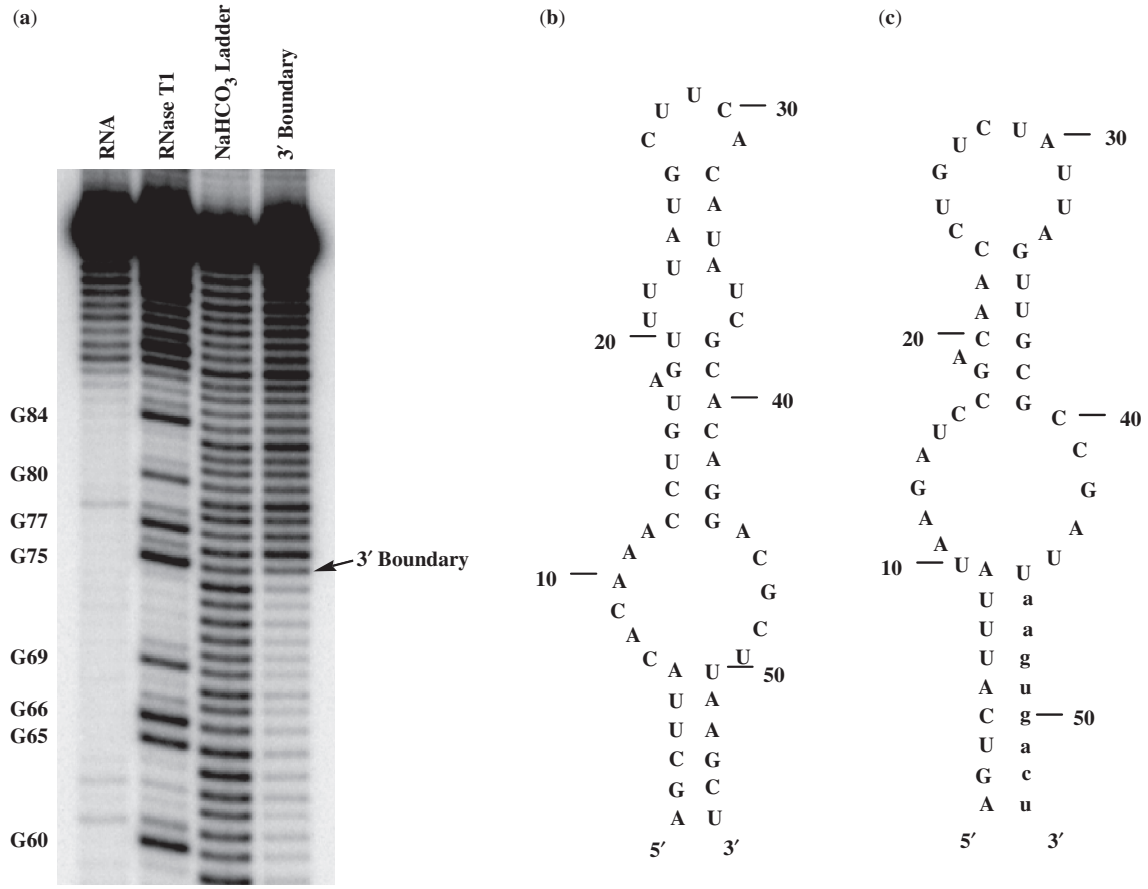

Figure 4. Engineering minimal aptamers. (**a**) Functional boundary determination for Aptamer M302. 3′-boundaries were determined by binding partially hydrolyzed, 5′-end-labeled Aptamer M302 to M3 HIV-1 RT. Recovered RNA fragments were analyzed by PAGE (lane 2), along with unreacted Aptamer M302 (lane 1), a partially hydrolyzed Aptamer M302 ladder (lane 3) and a G-ladder generated by nuclease T1 hydrolysis (lane 4). G75 is the functional 3′-boundary of Aptamer. (**b**) Predicted secondary structure of minimal Aptamer M302-S. (**c**) Predicted secondary structure of minimal Aptamer 12.01-S.

Residues U38-A47, C52-A61 and C68-U72 of Aptamer 12.01 were predicted to fall outside of paired stem structures, and were prone to NMIA modification by primer extension, largely confirming the prediction of Aptamer 12.01's secondary structure. Chemical probing by SHAPE of Aptamer M302 was also largely consistent with the predicted structure, in that A30-A34, A41, C49-A52 and A67-C71 were predicted to fall outside of base-paired regions. Residues U43, U44, U58 and C59 were also unreactive, possibly because these residues are involved in tertiary structural pairings or are otherwise sterically hindered. However, it is also possible that these residues are just continuation of the helix, since tandem U-U base pairs and U-C base pairs are observed in RNA crystal structures (36,37).

Boundary mapping experiments were also performed with Aptamers M302 and 12.01. For 3′-boundary mapping, (5′-^{32}P)-labeled RNA was used. After partial alkaline hydrolysis and binding to HIV-1 RT, functional RNA fragments were isolated by filtration, and the population of functional fragments was analyzed by PAGE. There was clearly a protein-binding 3′-boundary at G75 of M302 (Figure 4a), and a 5′-boundary was similarly mapped to C23 using (3′-^{32}P)-labeled RNA (data not shown). A 3′-boundary (U77) for Aptamer 12.01 was determined, but a 5′-boundary could not be delineated. The minimal requirements for Aptamer 12.01 were instead determined by synthesizing foreshortened constructs.

To confirm the boundaries of M302 and 12.01, minimal versions of the aptamers were designed and synthesized. Three more minimal versions of Aptamer M302 were constructed: M302-1, M302-2 and M302-S (Figure 4b) span nucleotides 25–75, 24–76 and 23–77, respectively, of the parental Aptamer M302, and also have AG substituted for the first two nucleotides and CU for the last two nucleotides (these substitutions facilitate enzymatic incorporation of biotin, for later applications). A standard binding assay (at 100 nM of M3 HIV-1 RT) revealed that all three foreshortened aptamers retained their activity, but that the longest aptamer, M302-S, had the best binding. Minimal versions of Aptamer 12.01 [12.01-1 (residues 33–77), 12.01-2 (32–78), 12.01-3 (31–79), 12.01-4 (30–80) and 12.01-S (29–81)] were also constructed (Figure 4c). Similar binding was observed for all five constructs, although the longest construct again had the best binding activity.

The affinities of the minimal aptamers 12.01-S and M302-S were also measured. As shown in Figure 4d,

both shortened aptamers have decreased binding affinities compared with their parental sequences. The dissociation constant of 12.01-S increased about 2-fold (from 70 to 120 nM for binding to WT HIV-1 RT, and from 70 to 15 nM for binding to M3 HIV-1 RT), while the dissociation constant of M302-S increased from 30 to 100 nM for M3 HIV-1 RT. The minimal M302-S variants had binding specificities for M3 HIV-1 RT relative to WT HIV-1 RT that were similar to the specificity of the longer, parental aptamer (Figure 5).

We and others have shown that aptamers can have extraordinary specificities for their targets. An aptamer isolated against theophylline can discriminate against caffeine by a factor of over 1000, even though caffeine differs from theophylline by a single methyl group (38). Aptamers that can bind to L-citrulline and L-arginine can discriminate between these two compounds and also their D-isomers (39). Aptamers can also finely discriminate between related proteins. An aptamer against the beta 2 isozyme of protein kinase C could readily distinguish it from the highly related alpha isozyme (40). The aptamer NX 1838 which was selected against the 165-amino-acid form of vascular endothelial growth factor (VEGF165) does not show any binding affinity to VEGF 121, which lacks exon 7 sequences (41). Finally, an anti-bFGF (basic fibroblast growth factor) aptamer discriminates against other members of the related FGF family (42). Perhaps, one of the best examples of aptamer discrimination between proteins, though, is the ability of aptamers to distinguish one species from another. An aptamer has been shown to separate bovine factor IX from human factor IX (43) Sullenger and co-workers (44) have actually used 'toggle selections' between species to identify aptamers that specifically recognize homologous proteins from one or another organism. An anti-porcine thrombin (FIIa) aptamer bound porcine FIIa with a dissociation constant of 50 ± 8 pM, but human FIIa with a dissociation constant of >600 nM, a $>10\,000$-fold change in affinity.

Specificities of anti-M3 aptamers

The dissociation constants of Aptamers 12.01 and M302 were determined by measuring binding as a function of protein concentration, for both M3 and WT HIV-1 RTs (Figure 5a and b). Surprisingly, despite the fact that negative selection was employed and the final pools appeared to discriminate between the protein variants, Aptamer 12.01 had a binding constant of 70 nM for both M3 and WT HIV-1 RTs. In contrast, Aptamer M302 had a binding constant for M3 HIV-1 RT of 30 nM, but bound the WT enzyme with an affinity similar to that of the unselected pool RNA (about 1 μM, Figure 5c). As a positive control, the dissociation constant of TPK1.1 for WT HIV-1 RT was also measured. The reported dissociation constant value is 5 nM, while we obtained a value of 14 nM (9); similar results were obtained both with our binding buffer and with the binding buffer described therein. TPK1.1 showed no binding above background to M3 HIV-1 RT (Figure 5d).

To further assess the specificity of M302, this aptamer was incubated with either 0.5 μM of M3 HIV-1 RT, WT HIV-1 RT, AMV RT or M-MLV RT in Selection Buffer. Of course, because AMV RT was used to reverse transcribe RNA to cDNA during the selection process, isolated aptamers should not be able to strongly bind to AMV RT. As shown in Figure 6, M302 specifically binds to M3 HIV-1 RT relative to RTs from other species of RTs. Such specificity has previously been demonstrated

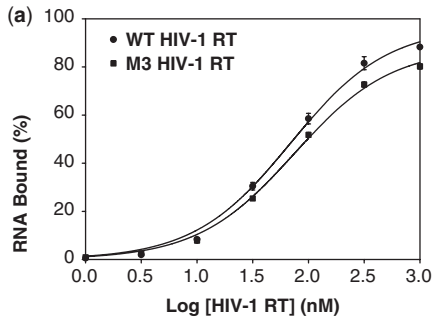

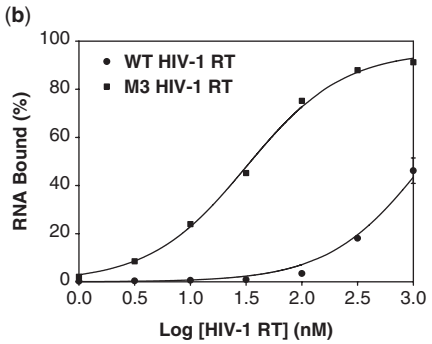

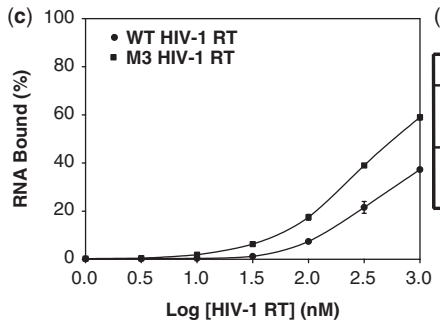

(d)

Aptamer		Pool	TPK1.1	12.01	12.01-S	M302	M302-S
Dissociation constant (nM)	WT	~1000	14	70	120	>1000	>1000
	M3	~1000	>1000	70	150	30	100
Inhibition constant (nM)	WT	>1000	10	>1000	>1000	>1000	>1000
	M3	>1000	>1000	>1000	>1000	>1000	>1000

Figure 5. Dissociation constants of anti-HIV-1 RT aptamers. (**a**) Binding curve of Aptamer 12.01 to M3 (squares) and WT (dots) HIV-1 RTs. (**b**) Binding curve of Aptamer M302 to M3 (squares) and WT (dots) HIV-1 RTs. (**c**) Binding curve of unselected pool RNA to M3 (squares) and WT (dots) HIV-1 RTs. (**d**) Summary of aptamers' binding constants (at 25°C) and inhibition constants (at 37°C). All values are in nanomolar.

for aptamers selected against HIV-1 RT, M-MLV RT and AMV RT (9,45).

In order to determine whether the aptamers might eventually be useful for *in vivo* applications, binding assays of isolated aptamers were also performed at 37°C and gave similar results. This is perhaps not surprising for TPK1.1, as it had been selected under a regime where it saw both 4°C and 37°C incubations (9), and had also been shown to form competent complexes with RT at room temperature (46). However, our aptamers have previously only been selected and assayed at ambient temperature, and thus it is interesting that they maintained performance at higher temperatures.

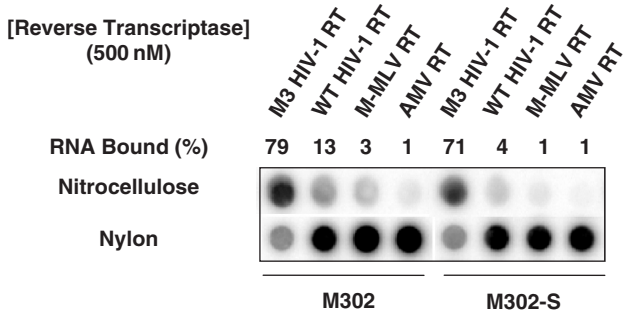

Figure 6. Binding specificities of anti-RT aptamers. Different reverse transcriptases (0.5 μM) were incubated with Aptamer M302 for 30 min in Selection Buffer at 25°C. Protein-bound RNA was retained on the nitrocellulose filter and free RNA flowed through to the nylon filter during vacuum filtration.

Aptamers bind but do not inhibit RTs

Wild-type HIV-1 RT has both DNA polymerase activity and RNase H activity. M3 HIV-1 RT has polymerase activity that is comparable to WT HIV-1 RT (Figure 7a), but has lost most of its RNase H activity (Figure 7b). This was somewhat unexpected since the amino acid substitutions in M3 were in the polymerase but not the RNase H domain. However, it is known that mutations in the polymerase domain can affect RNase H activity by affecting the position of the template-primer or the structure of the RNase H domain itself (47). The abilities of selected aptamers to inhibit the DNA polymerase activity of M3 and WT HIV-1 RTs were assayed at 37°C. Neither the aptamers nor unselected pool RNA was able to significantly inhibit the

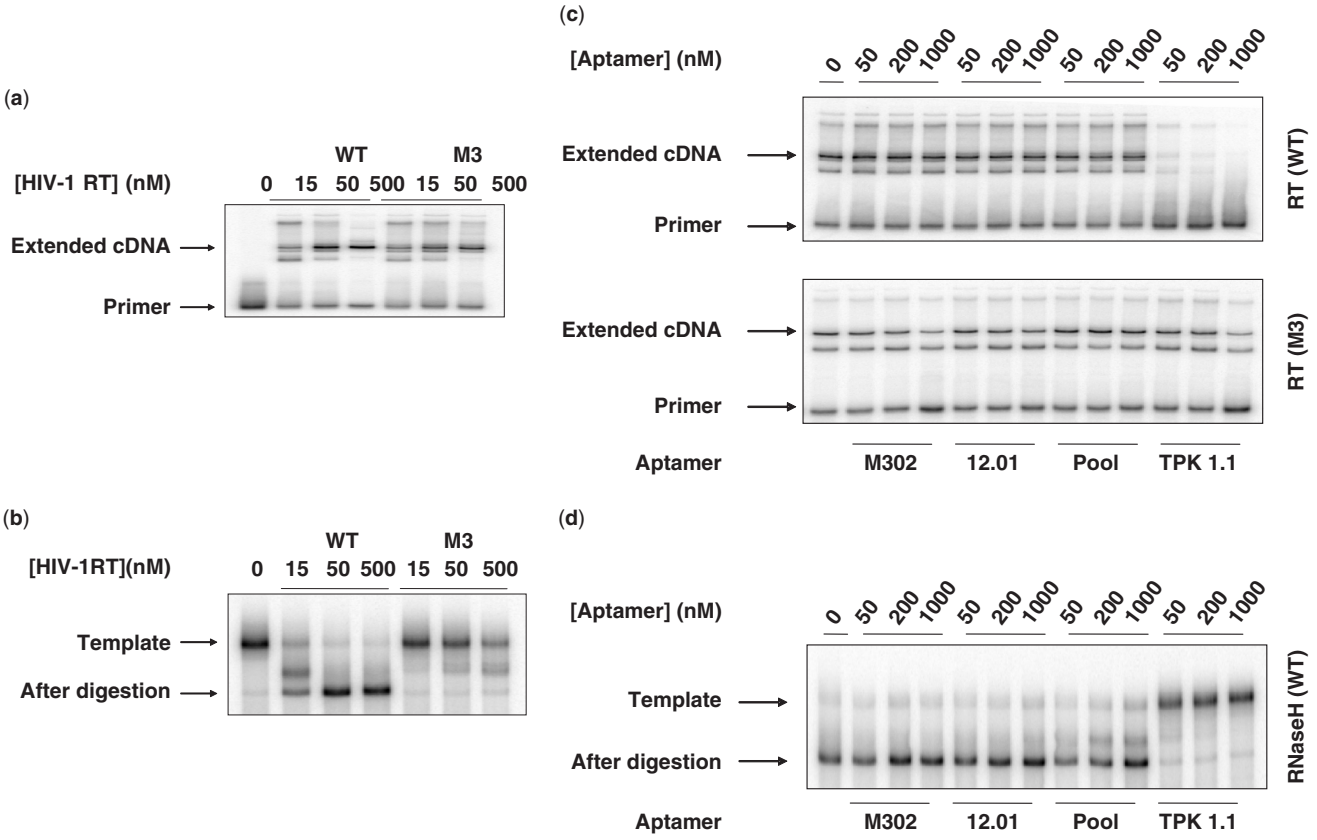

Figure 7. Inhibitory activities of anti-RT aptamers. (**a**) Polymerization activity of RTs. A (5′-^{32}P)-labeled primer was extended by M3 HIV-1 RT or by WT HIV-1 RT. Either 0, 15, 50 or 500 nM HIV-1 RT was used. Labeled primer and extended cDNA are denoted by arrows to the left. (**b**) RNase H activity of RTs. A (5′-^{32}P)-labeled template was digested by M3 HIV-1 RT or WT HIV-1 RT. M3 HIV-1 RT does not show obvious RNase H activity. Labeled template and degradation products are denoted by arrows to the left. (**c**) Aptamer inhibition of polymerase activity. Aptamer 12.01 and Aptamer M302 at varying concentrations (0, 50, 200, 1000 nM) were incubated with radiolabeled primer and an RNA template. Labeled primer and extended cDNA are denoted by arrows to the left. (**d**) Aptamer inhibition of RNase H activity. Aptamer 12.01 and Aptamer M302 at varying concentrations (0, 50, 200, 1000 nM) were incubated with radiolabeled primer and an RNA template. Labeled template and degradation products are denoted by arrows to the left.

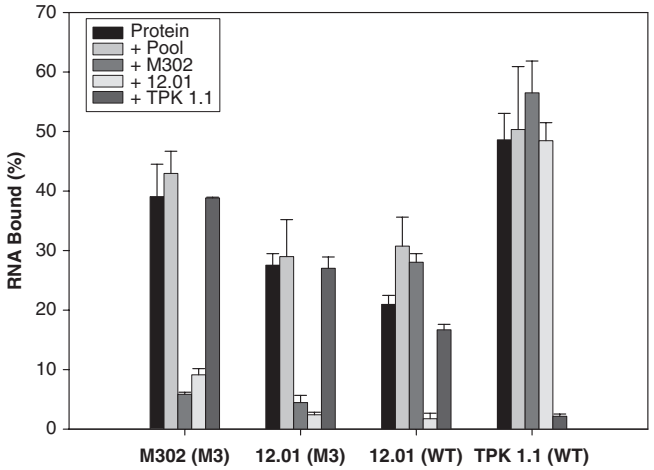

Figure 8. Competitive binding of aptamers to M3 and WT HIV-1 RTs. Aptamers M302, 12.01, TPK1.1 and the unselected pool RNA (N50) were end-labeled (all at 0.1 nM, indicated on *x*-axis) competed with different cold versions of the same RNAs (all at 1000 nM, indicated in inset) in the presence of either M3 or WT RT (indicated on *x*-axis). Bound, radiolabeled RNA was collected by filtration and quantitated.

extension of a (5′-^{32}P)-labeled primer up to concentrations of 1 μM. In contrast and as a positive control, TPK1.1 readily inhibited primer extension, as has been previously described (9). Similarly, the selected aptamers did not inhibit the RNase H activity of WT HIV-1 RT, although TPK1.1 again showed strong inhibition (Figure 7c) (14).

Anti-M3 aptamers recognize a unique epitope on HIV-1 RT

The fact that our selected aptamers bound but did not inhibit HIV-1 RTs suggested that they might bind in a different way or at a different site than the canonical pseudoknot aptamers that have previously been discovered. In order to determine whether the various aptamers were binding different protein epitopes, we carried out competitive binding assays. As can be seen in Figure 8, each of the aptamers 12.01 and M302 inhibits binding of the other to M3 HIV-1 RT. It is likely this is not due to interactions between the two RNAs, since M302 does not interfere with the binding of 12.01 to WT HIV-1 RT. In contrast, Aptamer 12.01 and TPK1.1 do not compete for binding to WT HIV-1 RT. These results are consistent with the activity assays described above, since TPK1.1 has been shown to bind to the template-primer binding site of WT HIV-1 RT (13,46,48,49) The simplest explanation of these results is that the binding sites for 12.01 and M302 on HIV-1 RTs are remote from the template-primer binding site. To our knowledge, this is the first pair of aptamers that recognize and bind to different epitopes on HIV-1 RT. Indeed, there have previously been only a few selections yielding aptamers that bound to more than one epitope on any protein (44,50–53).

Given that a number of previous selections have produced pseudoknot aptamers that bind to the template-primer binding site of HIV-1 RT, it is interesting that our selection produced a compact hairpin structure that bound to different, non-overlapping epitopes on the viral protein. The amino acid substitutions in M3 HIV-1 RT may impede binding of the canonical pseudoknot aptamer (TPK1.1) to RT's template-primer binding site, perhaps due to a conformational change in this site, and would similarly have made it less likely for this structure to be selected. In contrast, these substitutions might make a different epitope even more attractive during selection. For Aptamer M302, it is possible that the 8-amino-acid difference between WT and M3 HIV-1 RT induced a conformational change that yielded a M3-specific epitope that was readily recognized by RNA.

The recognition of a conformation-specific epitope is consistent with what is known of HIV-1 RT enzymology. Most of the TAMs are in the neighborhood of incoming nucleotides. These mutations may induce conformational changes in the dNTP-binding site and alter interactions with the 3′-azido group of AZT, thereby enhancing its excision (54). Substitutions that are not immediately adjacent to the nucleotide, such as M41L, may reinforce these conformational changes. In fact, treatment of HIV-1 infected patients with AZT induces two distinct patterns of resistance mutations. M3 HIV-1 RT contains the TAM-1 cluster, and also D67N, K70R, T215F and K219Q, some of which are representative of the TAM-2 cluster (55–57). While the structure of an AZT resistant RT with a TAM-2 cluster revealed that one or both of the substitutions T215F and K219Q might have induced long-range conformational changes in the RT active site, the crystal structure of RTs containing the M184V mutation either in the absence or in the presence of M41L and T215Y showed the polymerase active site had essentially the same conformation as did WT HIV-1 RT (58). However, the other substitutions found in M3 might cause conformational changes that could lead to rejection of TPK 1.1 or other aptamers from the template-primer-binding site. Indeed, it has been suggested that M184V and other amino acid residues involved in resistance to NRTI might affect the positioning or conformation of the template-primer (31,59).

The conformational epitope that is revealed on M3 HIV-1 RT may be very similar to one already found on the WT HIV-1 RT, since Aptamer M302 apparently recognizes a similar or overlapping epitope to that recognized by Aptamer 12.01 on both M3 and the WT protein. The RNase H domain is another possible binding site for aptamers, although to date aptamers directed solely against this portion have bound weakly (8,60,61). However, since Aptamer 12.01 does not inhibit the RNase H activity of WT HIV-1 RT, it is less likely that both Aptamers 12.01 and M302 bind to the RNase H domain.

Anti-M3 aptamers can be used in microarray-based sandwich assays

Aptamers have previously been adapted to a variety of assay formats for protein detection, including different types of sandwich assays (62). For sandwich assays, immobilized aptamers [anti-PDGF, anti-thrombin, anti-bFGF, anti-VEGF and anti-MUC1 (63)] capture target proteins which are in turn detected with either antibodies

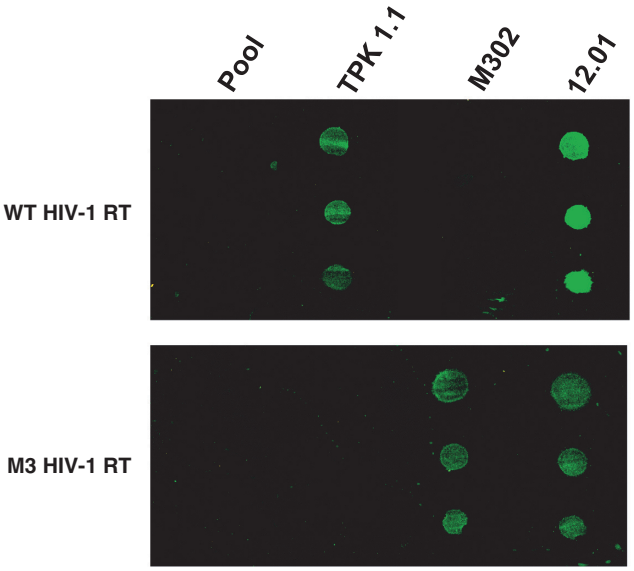

Figure 9. Specific detection of M3 versus WT RT by selected aptamers. Biotin-labeled aptamers were immobilized onto neutravidin-coated slides. Immobilized aptamers were sequentially incubated with M3 or WT HIV-1 RT, a polyclonal anti-HIV-1 RT antibody from rabbit and Cy3-labeled anti-rabbit IgG. The slide was scanned for fluorescence on a microarray scanner—GenePix 4000 B.

or a second aptamer (62). Recently, an antibody-protein-aptamer format has been demonstrated for the protein dimer PDGF (64). Given that we have selected aptamers appear to have different binding specificity to closely related WT and M3 HIV-1 RTs, we wished to see if this property would also hold true in a facile sandwich assay. In order to assess this hypothesis, we reamplified the DNA templates of M302, 12.01, TPK1.1 and the N50 pool using primers containing a T7 RNA polymerase phi 2.5 promoter, which replaces the initiating G with A. Using the reconstructed DNA templates, we initiated transcription with biotin-AMP (65). The yield of biotinylated aptamers was about 40% by streptavidin gel-shift assay. 5′-biotinlyated RNA was immobilized onto neutravidin-coated slides and incubated with either WT or M3 HIV-1 RTs. After washing, an anti-HIV-1 RT primary antibody from rabbit and Cy3-labeled anti-rabbit IgG secondary antibody were sequentially applied to detect captured proteins on the array.

Using this sandwich assay, we found we could sensitively detect M3 and WT HIV-1 RTs spiked into complex biological fluids (Blocking Buffer) at concentrations as low as 1 nM (Figure 9). The specificities available with our and others' selected aptamers led to specific identification of the protein variants, with Aptamer M302 detecting only M3 HIV-1 RT, TPK1.1 detecting only WT HIV-1 RT, and Aptamer 12.01 detecting both. While optimization of these arrays will be necessary for quantitative determination of RT, further expansion of the number of aptamers that recognize drug-resistant RT variants could lead to the development of protein-detection arrays that could finely discriminate between the shapes of different RT variants. This would open the way to using aptamers for directly screening for drug resistance, including by augmenting current genotyping assays. That said, we recognize that it is an open question whether or not aptamers can not only discriminate based on shape, but can also classify based on shape. This is an interesting question that we hope to resolve into the future.

ACKNOWLEDGEMENTS

Dr Ellington would like to thank the Welch Foundation for their continued support.

FUNDING

The National Institutes of Health (Sub-grant # 9-526-1123 of 5 P01-AI061797). Funding for open access charge: The National Institutes of Health (Sub-grant # 9-526-1123 of 5 P01-AI061797).

Conflict of interest statement. None declared.

REFERENCES

1. Piacenti,F.J. (2006) An update and review of antiretroviral therapy. *Pharmacotherapy*, **26**, 1111–1133.
2. Johnson,V.A., Brun-Vezinet,F., Clotet,B., Gunthard,H.F., Kuritzkes,D.R., Pillay,D., Schapiro,J.M. and Richman,D.D. (2008) Update of the drug resistance mutations in HIV-1: spring 2008. *Top. HIV Med.*, **16**, 62–68.
3. Mansky,L.M. and Temin,H.M. (1995) Lower in vivo mutation rate of human immunodeficiency virus type 1 than that predicted from the fidelity of purified reverse transcriptase. *J. Virol.*, **69**, 5087–5094.
4. Perelson,A.S., Neumann,A.U., Markowitz,M., Leonard,J.M. and Ho,D.D. (1996) HIV-1 dynamics in vivo: virion clearance rate, infected cell life-span, and viral generation time. *Science*, **271**, 1582–1586.
5. Hirsch,M.S., Günthard,H.F., Schapiro,J.M., Brun-Vézinet,F., Clotet,B., Hammer,S.M., Johnson,V.A., Kuritzkes,D.R., Mellors,J.W., Pillay,D. *et al.* (2008) Antiretroviral drug resistance testing in adult HIV-1 infection: 2008 recommendations of an International AIDS Society-USA panel. *Clin. Infect. Dis.*, **47**, 266–285.
6. Little,S.J., Holte,S., Routy,J.P., Daar,E.S., Markowitz,M., Collier,A.C., Koup,R.A., Mellors,J.W., Connick,, E. Conway,B. *et al.* (2002) Antiretroviral-drug resistance among patients recently infected with HIV. *NEJM*, **347**, 385–394.
7. Shet,A., Berry,L., Mohri,H., Mehandru,S., Chung,C., Kim,A., Jean-Pierre,P., Hogan,C., Simon,V., Boden,D. *et al.* (2006) Tracking the prevalence of transmitted antiretroviral drug-resistant HIV-1: a decade of experience. *J. Acquir. Immune. Defic. Syndr.*, **41**, 439–446.
8. Held,D.M., Kissel,J.D., Patterson,J.T., Nickens,D.G. and Burke,D.H. (2006) HIV-1 inactivation by nucleic acid aptamers. *Front. Biosci.*, **11**, 89–112 [Review].
9. Tuerk,C., MacDougal,S. and Gold,L. (1992) RNA pseudoknots that inhibit human immunodeficiency virus type 1 reverse transcriptase. *Proc. Natl Acad. Sci. USA*, **89**, 6988–6992.
10. Burke,D.H., Scates,L., Andrews,K. and Gold,L. (1996) Bent pseudoknots and novel RNA inhibitors of type 1 human immunodeficiency virus (HIV-1) reverse transcriptase. *J. Mol. Biol.*, **264**, 650–666.
11. Schneider,D.J., Feigon,J., Hostomsky,Z. and Gold,L. (1995) High-affinity ssDNA inhibitors of the reverse transcriptase of type 1 human immunodeficiency virus. *Biochemistry*, **34**, 9599–9610.
12. de Soultrait,V.R., Caumont,A., Parissi,V., Morellet,N., Ventura,M., Lenoir,C., Litvak,S., Fournier,M. and Roques,B. (2002) A novel short peptide is a specific inhibitor of the human immunodeficiency virus type 1 integrase. *J. Mol. Biol.*, **318**, 45–58.

13. Joshi,P. and Prasad,V.R. (2002) Potent inhibition of human immunodeficiency virus type 1 replication by template analog reverse transcriptase inhibitors derived by SELEX (systematic evolution of ligands by exponential enrichment). *J. Virol.*, **76**, 6545–6557.
14. Held,D.M., Kissel,J.D., Thacker,S.J., Michalowski,D., Saran,D., Ji,J., Hardy,R.W., Rossi,J.J. and Burke,D.H. (2007) Cross-clade inhibition of recombinant human immunodeficiency virus type 1 (HIV-1), HIV-2, and simian immunodeficiency virus SIVcpz reverse transcriptases by RNA pseudoknot aptamers. *J. Virol.*, **81**, 5375–5384.
15. Kissel,J.D., Held,D.M., Hardy,R.W. and Burke,D.H. (2007) Single-stranded DNA aptamer RT1t49 inhibits RT polymerase and RNase H functions of HIV type 1, HIV type 2, and SIVCPZ RTs. *AIDS Res. Hum. Retrovir.*, **23**, 699–708.
16. Fisher,T.S. and Prasad,V.R. (2002) Substitutions of Phe61 located in the vicinity of template 5′-overhang influence polymerase fidelity and nucleoside analog sensitivity of HIV-1 reverse transcriptase. *J. Biol. Chem.*, **277**, 22345–22352.
17. Fisher,T.S., Joshi,P. and Prasad,V.R. (2005) HIV-1 reverse transcriptase mutations that confer decreased in vitro susceptibility to anti-RT DNA aptamer RT1t49 confer cross resistance to other anti-RT aptamers but not to standard RT inhibitors. *AIDS Res. Ther.*, **2**, 8.
18. Sen,S., Tripathy,S.P. and Paranjape,R.S. (2006) Antiretroviral drug resistance testing. *J. Postgrad. Med.*, **52**, 187–193.
19. Collett,J.R., Cho,E.J., Lee,J.F., Levy,M., Hood,A.J., Wan,C. and Ellington,A.D. (2005) Functional RNA microarrays for high-throughput screening of antiprotein aptamers. *Anal. Biochem.*, **338**, 113–123.
20. Cho,E.J., Collett,J.R., Szafranska,A.E. and Ellington,A.D. (2006) Optimization of aptamer microarray technology for multiple protein targets. *Anal. Chim. Acta*, **564**, 82–90.
21. Hou,E.W., Prasad,R., Beard,W.A. and Wilson,S.H. (2004) High-level expression and purification of untagged and histidine-tagged HIV-1 reverse transcriptase. *Protein Expr. Purif.*, **34**, 75–86.
22. Merino,E.J., Wilkinson,K.A., Coughlan,J.L. and Weeks,K.M. (2005) RNA structure analysis at single nucleotide resolution by selective 2'-hydroxyl acylation and primer extension (SHAPE). *J. Am. Chem. Soc.*, **127**, 4223–4231.
23. Johnston,E., Dupnik,K.M., Gonzales,M.J., Winters,M.A., Rhee,S.Y., Imamichi,T. and Shafer,R.W. (2005) Panel of prototypical infectious molecular HIV-1 clones containing multiple nucleoside reverse transcriptase inhibitor resistance mutations. *AIDS*, **19**, 731–733.
24. Gonzales,M.J., Johnson,E., Dupnik,K.M., Imamichi,T. and Shafer,R.W. (2003) Colinearity of reverse transcriptase inhibitor resistance mutations detected by population-based sequencing. *J. Acquir. Immune. Defic. Syndr.*, **34**, 398–402.
25. Larder,B.A. and Kemp,S.D. (1989) Multiple mutations in HIV-1 reverse transcriptase confer high-level resistance to zidovudine (AZT). *Science*, **246**, 1155–1158.
26. Kellam,P., Boucher,C.A. and Larder,B.A (1992) Fifth mutation in human immunodeficiency virus type 1 reverse transcriptase contributes to the development of high-level resistance to zidovudine. *Proc. Natl Acad. Sci. USA*, **89**, 1934–1938.
27. Romano,L., Venturi,G., Bloor,S., Harrigan,R., Larder,B.A., Major,J.C. and Zazzi,M. (2002) Broad nucleoside-analogue resistance implications for human immunodeficiency virus type 1 reverse-transcriptase mutations at codons 44 and 118. *J. Infect. Dis.*, **185**, 898–904.
28. Girouard,M., Diallo,K., Marchand,B., McCormick,S. and Götte,M. (2003) Mutations E44D and V118I in the reverse transcriptase of HIV-1 play distinct mechanistic roles in dual resistance to AZT and 3TC. *J. Biol. Chem.*, **278**, 34403–34410.
29. Tisdale,M., Kemp,S.D., Parry,N.R. and Larder,B.A. (1993) Rapid in vitro selection of human immunodeficiency virus type 1 resistant to 3'-thiacytidine inhibitors due to a mutation in the YMDD region of reverse transcriptase. *Proc. Natl Acad. Sci. USA*, **90**, 5653–5656.
30. Götte,M., Arion,D., Parniak,M.A. and Wainberg,M.A. (2000) The M184V mutation in the reverse transcriptase of human immunodeficiency virus type 1 impairs rescue of chain-terminated DNA synthesis. *J. Virol.*, **74**, 3579–3585.
31. Boyer,P.L., Sarafianos,S.G., Arnold,E. and Hughes,S.H. (2002) The M184V mutation reduces the selective excision of zidovudine 5′-monophosphate (AZTMP) by the reverse transcriptase of human immunodeficiency virus type 1. *J. Virol.*, **76**, 3248–3256.
32. Tuerk,C., Eddy,S., Parma,D. and Gold,L. (1990) Autogenous translational operator recognized by bacteriophage T4 DNA polymerase. *J. Mol. Biol.*, **213**, 749–761.
33. Bailey,T.L. and Elkan,C. (1994) Fitting a mixture model by expectation maximization to discover motifs in biopolymers. *Proc. Int. Conf. Intell. Syst. Mol. Biol.*, **2**, 28–36.
34. Zuker,M., Mathews,D.H. and Turner,D.H. (1999) Algorithms and thermodynamics for RNA secondary structure prediction: a practical guide. In Barciszewski,J. and Clark,B.F.C. (eds), *RNA Biochemistry and Biotechnology,* Vol. 70, NATO ASI Series. Kluwer Academic Publishers, Netherlands, pp. 11–44.
35. Wilkinson,K.A., Merino,E.J. and Weeks,K.M. (2005) RNA SHAPE chemistry reveals nonhierarchical interactions dominate equilibrium structural transitions in tRNA(Asp) transcripts. *J. Am. Chem. Soc.*, **127**, 4659–4667.
36. Holbrook,S.R., Cheong,C., Tinoco,I. Jr. and Kim,S.H. (1991) Crystal structure of an RNA double helix incorporating a track of non-Watson–Crick base pairs. *Nature*, **353**, 579–581.
37. Baeyens,K.J., De Bondt,H.L. and Holbrook,S.R. (1995) Structure of an RNA double helix including uracil-uracil base pairs in an internal loop. *Nat. Struct. Biol.*, **2**, 56–62.
38. Jenison,R.D., Gill,S.C., Pardi,A. and Polisky,B. (1994) High-resolution molecular discrimination by RNA. *Science*, **263**, 1425–1429.
39. Famulok,M. (1994) Molecular recognition of amino acids by RNA-aptamers: an L-citrulline binding RNA motif and its evolution into an L-arginine binder. *J. Am. Chem. Soc.*, **116**, 1698–1706.
40. Conrad,R., Keranen,L.M., Ellington,A.D. and Newton,A.C. (1994) Isozyme-specific inhibition of protein kinase C by RNA aptamers. *J. Biol. Chem.*, **269**, 32051–32054.
41. Ruckman,J., Green,L.S., Beeson,J., Waugh,S., Gillette,W.L., Henninger,D.D., Claesson-Welsh,L. and Janjić,N. (1998) 2'-Fluoropyrimidine RNA-based aptamers to the 165-amino acid form of vascular endothelial growth factor (VEGF165). Inhibition of receptor binding and VEGF-induced vascular permeability through interactions requiring the exon 7-encoded domain. *J. Biol. Chem.*, **273**, 20556–20567.
42. Jellinek,D., Green,L.S., Bell,C., Lynott,C.K., Gill,N., Vargeese,C., Kirschenheuter,G., McGee,D.P., Abesinghe,P., Pieken,W.A. *et al.* (1995) Potent 2'-amino-2'-deoxypyrimidine RNA inhibitors of basic fibroblast growth factor. *Biochemistry*, **34**, 11363–11372.
43. Gopinath,S.C., Balasundaresan,D., Akitomi,J. and Mizuno,H. (2006) An RNA aptamer that discriminates bovine factor IX from human factor IX. *J. Biochem.*, **140**, 667–676.
44. White,R., Rusconi,C., Scardino,E., Wolberg,A., Lawson,J., Hoffman,M. and Sullenger,B. (2001) Generation of species cross-reactive aptamers using "toggle" SELEX. *Mol. Ther.*, **4**, 567–573.
45. Chen,H. and Gold,L. (1994) Selection of high-affinity RNA ligands to reverse transcriptase: inhibition of cDNA synthesis and RNase H activity. *Biochemistry*, **33**, 8746–8756.
46. Jaeger,J., Restle,T. and Steitz,T.A. (1998) The structure of HIV-1 reverse transcriptase complexed with an RNA pseudoknot inhibitor. *EMBO J.*, **17**, 4535–4542.
47. Gao,H.Q., Boyer,, P.L. Arnold,E. and Hughes,S.H. (1998) Effects of mutations in the polymerase domain on the polymerase, RNase H and strand transfer activities of human immunodeficiency virus type 1 reverse transcriptase. *J. Mol. Biol.*, **277**, 559–572.
48. Wöhrl,B.M., Krebs,R., Goody,R.S. and Restle,T. (1999) Refined model for primer/template binding by HIV-1 reverse transcriptase: pre-steady-state kinetic analyses of primer/template binding and nucleotide incorporation events distinguish between different binding modes depending on the nature of the nucleic acid substrate. *J. Mol. Biol.*, **292**, 333–344.
49. Held,D.M., Kissel,J.D., Saran,D., Michalowski,D. and Burke,D.H. (2006) Differential susceptibility of HIV-1 reverse transcriptase to inhibition by RNA aptamers in enzymatic reactions monitoring specific steps during genome replication. *J. Biol. Chem.*, **281**, 25712–25722.
50. Macaya,R.F., Waldron,J.A., Beutel,B.A., Gao,H., Joesten,M.E., Yang,M., Patel,R., Bertelsen,A.H. and Cook,A.F. (1995) Structural

and functional characterization of potent antithrombotic oligonucleotides possessing both quadruplex and duplex motifs. *Biochemistry*, **34**, 4478–4492.
51. Tasset,D.M., Kubik,M.F. and Steiner,W. (1997) Oligonucleotide inhibitors of human thrombin that bind distinct epitopes. *J. Mol. Biol.*, **272**, 688–698.
52. Hicke,B.J., Marion,C., Chang,Y.F., Gould,T., Lynott,C.K., Parma,D., Schmidt,P.G. and Warren,S. (2001) Tenascin-C aptamers are generated using tumor cells and purified protein. *J. Biol. Chem.*, **276**, 48644–48654.
53. Chen,C.H., Chernis,G.A., Hoang,V.Q. and Landgraf,R. (2003) Inhibition of heregulin signaling by anaptamer that preferentially binds to the oligomeric form of human epidermal growth factor receptor-3. *Proc. Natl Acad. Sci. USA*, **100**, 9226–9231.
54. Sarafianos,S.G., Das,K., Ding,J., Boyer,P.L., Hughes,S.H. and Arnold,E. (1999) Touching the heart of HIV-1 drug resistance: the fingers close down on the dNTP at the polymerase active site. *Chem. Biol.*, **6**, R137–R146.
55. Yahi,N., Tamalet,C., Tourrès,C., Tivoli,N., Ariasi,F., Volot,F., Gastaut,J.A., Gallais,H., Moreau,J. and Fantini,J. (1999) Mutation patterns of the reverse transcriptase and protease genes in human immunodeficiency virus type 1-infected patients undergoing combination therapy: survey of 787 sequences. *J. Clin. Microbiol.*, **37**, 4099–4106.
56. Hanna,G.J., Johnson,V.A., Kuritzkes,D.R., Richman,D.D., Brown,A.J., Savara,A.V., Hazelwood,J.D. and D'Aquila,R.T. (2000) Patterns of resistance mutations selected by treatment of human immunodeficiency virus type 1 infection with zidovudine, didanosine, and nevirapine. *J. Infect. Dis.*, **181**, 904–911.
57. Marcelin,A.G., Delaugerre,C., Wirden,M., Viegas,P., Simon,A., Katlama,C. and Calvez,V. (2004) Thymidine analogue reverse transcriptase inhibitors resistance mutations profiles and association to other nucleoside reverse transcriptase inhibitors resistance mutations observed in the context of virological failure. *J. Med. Virol.*, **72**, 162–165.
58. Chamberlain,P.P., Ren,J., Nichols,C.E., Douglas,L., Lennerstrand,J., Larder,B.A., Stuart,D.I. and Stammers,D.K. (2002) Crystal structures of Zidovudine- or Lamivudine-resistant human immunodeficiency virus type 1 reverse transcriptases containing mutations at codons 41, 184, and 215. *J. Virol.*, **76**, 10015–10019.
59. Tantillo,C., Ding,J., Jacobo-Molina,A., Nanni,R.G., Boyer,P.L., Hughes,S.H., Pauwels,R., Andries,K., Janssen,P.A. and Arnold,E. (1994) Locations of anti-AIDS drug binding sites and resistance mutations in the three-dimensional structure of HIV-1 reverse transcriptase. Implications for mechanisms of drug inhibition and resistance. *J. Mol. Biol.*, **243**, 369–387.
60. Hannoush,R.N., Carriero,S., Min,K.L. and Damha,M.J. (2004) Selective inhibition of HIV-1 reverse transcriptase (HIV-1 RT) RNase H by small RNA hairpins and dumbbells. *Chembiochem*, **5**, 527–533.
61. Andreola,M.L., Pileur,F., Calmels,C., Ventura,M., Tarrago-Litvak,L., Toulmé,J.J. and Litvak,S. (2001) DNA aptamers selected against the HIV-1 RNase H display in vitro antiviral activity. *Biochemistry*, **40**, 10087–10094.
62. Tombelli,S., Minunni,M. and Mascini,M. (2007) Aptamers-based assays for diagnostics, environmental and food analysis. *Biomol. Eng.*, **24**, 191–200.
63. Ferreira,C.S., Papamichael,K., Guilbault,G., Schwarzacher,T., Gariepy,J. and Missailidis,S. (2008) DNA aptamers against the MUC1 tumour marker: design of aptamer-antibody sandwich ELISA for the early diagnosis of epithelial tumours. *Anal. Bioanal. Chem.*, **390**, 1039–1050.
64. Huang,Y., Nie,X.M., Gan,S.L., Jiang,J.H., Shen,G.L. and Yu,R.Q. (2008) Electrochemical immunosensor of platelet-derived growth factor with aptamer-primed polymerase amplification. *Anal. Biochem.*, **382**, 16–22.
65. Huang,F., Wang,G., Coleman,T. and Li,N. (2003) Synthesis of adenosine derivatives as transcription initiators and preparation of 5′ fluorescein- and biotin-labeled RNA through one-step in vitro transcription. *RNA*, **9**, 1562–1570.